ARR No. 3F25

NATIONAL ADVISORY COMMITTEE FOR AERONAUTICS

WARTIME REPORT

ORIGINALLY ISSUED
June 1943 as
Advance Restricted Report 3F25

EFFECT OF WING LOADING AND ALTITUDE ON LATERAL STABILITY AND CONTROL CHARACTERISTICS OF AN AIRPLANE AS DETERMINED BY TESTS OF A MODEL IN THE FREE-FLIGHT TUNNEL

By John P. Campbell and Charles L. Seacord, Jr.

Langley Memorial Aeronautical Laboratory
Langley Field, Va.

NACA

WASHINGTON

NATIONAL ADVISORY COMMITTEE FOR AERONAUTICS

ADVANCE RESTRICTED REPORT

EFFECT OF WING LOADING AND ALTITUDE ON LATERAL STABILITY AND CONTROL CHARACTERISTICS OF AN AIRPLANE AS DETERMINED BY TESTS OF A MODEL IN THE FREE-FLIGHT TUNNEL

By John P. Campbell and Charles L. Seacord, Jr.

SUMMARY

An investigation to determine the effects of wing loading and altitude on lateral stability and control has been carried out in the NACA free-flight tunnel. The results of flight tests of the model were correlated with calculated stability boundaries, and an effort was made to determine for each loading condition the airplane configuration that gave the best flight characteristics.

By changing the weight of the model, the relative density was varied to represent airplane wing loadings of 16 to 90 pounds per square foot at sea level or lighter loads at altitude. The dihedral angle was varied from 0° to 11.5° and the vertical-tail area from 3.5 to 14 percent of the wing area.

The tests showed that increasing wing loading and altitude did not affect spiral stability but reduced oscillatory stability, increased the difficulty of maintaining wing-level flight, and caused the general flight behavior to become worse. The best flight characteristics at all loadings were obtained with conditions of small dihedral and large vertical-tail area.

INTRODUCTION

Recent military airplane design trends have been toward increased wing loading and increased ceiling. These changes combine to cause increases in the factor μ, the ratio of airplane density to air density, because this factor varies directly with both wing loading and altitude. Recent theoretical papers (references 1 and 2) have pointed

out that difficulty may be experienced in obtaining dynamic lateral stability with airplanes having large values of μ. These papers indicate that the instability takes the form of the Dutch roll, a combined rolling and sideslipping oscillation, and that it is associated with high values of the wing dihedral angle and low vertical-tail area.

In an effort to obtain experimental correlation with these theoretical results and to determine the combinations of vertical-tail area and dihedral angle that give the best flying qualities for each loading, flight tests of a model of a typical fighter airplane with propeller removed and split flaps deflected 60° have been carried out in the NACA free-flight tunnel. The results of this investigation are given herein.

The flight investigation consisted in tests of the model in which the wing loading was varied to represent values of μ from 5.5 to 31.5. These values of μ correspond to wing loadings from 16 to 90 pounds per square foot for the airplane at sea level or from 6 to 34 pounds per square foot at 30,000 feet.

For each of the loading conditions of the model, the vertical-tail area and the dihedral angle were varied over a range of values representative of present-day airplane configurations.

The results of the flight tests of the model have been correlated with stability boundaries calculated for the particular model tested. Ratings for spiral stability, oscillatory stability, and general flight behavior are given for each condition of the model.

SYMBOLS

C_L lift coefficient (L/qS)

C_Y lateral-force coefficient (Y/qS)

C_n yawing-moment coefficient $\left(\frac{\text{yawing moment}}{qbS}\right)$

C_l rolling-moment coefficient $\left(\frac{\text{rolling moment}}{qbS}\right)$

L lift, pounds

Y lateral force, pounds

ρ_o mass density of air at standard sea-level conditions, slugs per cubic foot

ρ mass density of air at flight conditions, slugs per cubic foot

b wing span, feet

S wing area, square feet

S_v vertical-tail area, square feet

q dynamic pressure, pounds per square foot $(1/2\rho V^2)$

α angle of attack, degrees

V airspeed, feet per second

C_{Y_β} rate of change of lateral-force coefficient with sideslip, per radian $(\partial C_Y/\partial\beta)$

C_{n_β} rate of change of yawing-moment coefficient with sideslip, per radian $(\partial C_n/\partial\beta)$

C_{l_β} rate of change of rolling-moment coefficient with sideslip, per radian $(\partial C_l/\partial\beta)$

C_{n_p} rate of change of yawing-moment coefficient with rolling velocity, per unit of $pb/2V$ $\left(\partial C_n/\partial\frac{pb}{2V}\right)$

C_{l_p} rate of change of rolling-moment coefficient with rolling velocity, per unit of $pb/2V$ $\left(\partial C_l/\partial\frac{pb}{2V}\right)$

C_{l_r} rate of change of rolling-moment coefficient with yawing velocity, per unit of $rb/2V$ $\left(\partial C_l/\partial\frac{rb}{2V}\right)$

C_{n_r} rate of change of yawing-moment coefficient with yawing velocity, per unit of $rb/2V$ $\left(\partial C_n/\partial\frac{rb}{2V}\right)$

β angle of sideslip, radians

p rolling angular velocity, radians per second

r	yawing angular velocity, radians per second
A	aspect ratio (b^2/S)
μ	airplane relative-density factor ($m/\rho Sb$)
m	mass, slugs (W/g)
g	acceleration of gravity, feet per second per second
W	weight of airplane, pounds
W/S	wing loading of airplane, pounds per square foot
γ	angle of flight path to horizontal, degrees
Γ	dihedral angle, degrees
k_X/b	ratio of radius of gyration about X axis to wing span
k_Z/b	ratio of radius of gyration about Z axis to wing span
R	Routh's discriminant
E	coefficient in stability quartic equation, given in reference 1

(All coefficients are referred to stability axes.)

MODEL

Two similar 1/18-scale models, one of light and one of heavy construction, were used for the tests to permit large changes in wing loading. A drawing of the models as tested is shown in figure 1.

Both models were so constructed that weight, dihedral angle, and vertical-tail area could be changed without affecting the center of gravity or the radii of gyration. The light model, representing a wing loading of 16 pounds per square foot, was constructed of balsa; whereas the heavy model, representing wing loadings from 30 to 90 pounds per square foot, was built principally of spruce and plywood.

Both models were equipped with split flaps with chords 20 percent of the wing chord. The split flaps, which extended from the fuselage to the ailerons, were deflected 60°. The controls were electrically operated by a "pilot" in the same manner as those described in reference 3. The ratios of the radii of gyration to the wing span were held constant at $\frac{k_X}{b} = 0.143$ and $\frac{k_Z}{b} = 0.202$, and the center of gravity was held at 33 percent of the mean aerodynamic chord.

MEASUREMENT OF SIDESLIP DERIVATIVES

The sideslip derivatives C_{l_β}, C_{n_β}, and C_{Y_β} were determined for the different combinations of vertical-tail area and dihedral angle by tests on the six-component balance in the NACA free-flight tunnel. All the tests were made at an angle of attack of 8°, corresponding to a lift coefficient of 1.0, and at a dynamic pressure of 4.09 pounds per square foot. The derivatives were calculated from the slopes of the curves of C_l, C_n, and C_Y plotted against angle of yaw. The values of C_{l_β} and C_{n_β} for the combinations of dihedral angle and vertical-tail area are indicated in figure 2.

CALCULATION OF LATERAL-STABILITY BOUNDARIES

The calculated lateral-stability boundaries are given in figure 3 for the four values of μ used in the flight tests of the model. The boundaries, which are the loci of points of neutral spiral stability ($E = 0$) and neutral oscillatory stability ($R = 0$) at a lift coefficient of 1.0, were calculated by using the methods of reference 1, which were based upon the standard stability equations developed in reference 4. The boundary curves represent a simultaneous variation of the stability derivatives as given in table I. It will be noticed that the boundaries for $R = 0$ move upward and inward on the lateral-stability diagram as μ is increased. A single $E = 0$ boundary, however, was obtained for all values of μ used; this result indicates that spiral stability does not change with μ.

The lateral-stability boundaries were obtained by assuming various ratios of vertical-tail area to wing area S_v/S and, for each of these ratios, finding the values of C_{l_β} for which $E = 0$ and for which $R = 0$. The derivatives C_{l_p}, C_{n_p}, and C_{l_r} were found from the charts of reference 5. The contribution of the vertical tail to C_{n_r} was computed by the method of reference 1. The values of $\Delta C_{Y_{\beta(fin)}}$ required for this computation and the variation of C_{n_β} and C_{Y_β} with tail area were obtained from the force tests previously mentioned herein. The value of C_{n_r} for the model with the vertical tail removed was estimated from measured data for a similar model.

FLIGHT TESTS

The flight tests were made in the NACA free-flight tunnel, which is described in reference 3. All the tests for dynamic lateral stability and control were made at a lift coefficient of 1.0. For the range of wing loadings covered, the airspeeds required for flight at this lift coefficient varied from 28 to 66 feet per second.

The spiral stability of the model was determined by the pilot from the rate at which the model, with controls fixed, sideslipped and rolled from level flight.

Oscillatory-stability tests consisted in starting a lateral oscillation by an abrupt movement of the rudder while the model was in laterally level flight. Motion pictures of the flights were made in an effort to measure the period and damping of the ensuing oscillation; however, the flights during which the oscillation was not interrupted by control movements were seldom long enough for the damping of the oscillation to be accurately determined from the motion-picture records. Visual observations of the damping were also made, therefore, to supplement the motion-picture records.

The lateral control was judged by the difficulty with which wing-level flight was maintained, both with ailerons and rudder used together and with ailerons alone. During the flights with aileron alone the yawing due to aileron deflection was noted. The amount of this yawing and the

manner in which the model returned to neutral was taken as an indication of the directional stability.

An over-all flight-behavior rating based on the pilot's opinion of the general nature of the flights was recorded for each condition. The factors influencing these ratings included spiral stability, the type of the lateral oscillation, lateral control, and directional stability.

RESULTS AND DISCUSSION

Interpretation of Results

The results are given in terms of actual airplane wing loading at sea level, as the tests were made at standard sea-level conditions. Inasmuch as μ is directly proportional to both wing loading and altitude, the data given can be applied to airplanes flying at higher altitudes; that is, an airplane with an actual wing loading of 34 pounds per square foot flying at an altitude of 30,000 feet, where $\frac{\rho}{\rho_o} = 0.38$, will have the same stability characteristics as a similar airplane with a wing loading of 90 pounds per square foot flying at sea level. The variation of μ with effective wing loading and altitude is shown in figure 4.

Although the results were obtained for a model with flaps deflected and without a propeller, a wide range of stability derivatives was covered by varying the vertical-tail area and the dihedral angle. The results apply to any airplane having these particular stability derivatives regardless of the airplane configuration. The conclusions regarding the effect of μ on lateral stability and control, however, are believed to have general application.

Lateral Stability

Spiral stability.- In the flights no change in spiral stability with change in μ was observed. This result was in agreement with the theoretical stability calculations.

Average spiral-stability ratings from flight tests at

different values of μ are shown in figure 5, which is a lateral-stability diagram (C_{n_β} against $-C_{l_\beta}$) on which the spiral-stability boundary from figure 3 has been located. The ratings are placed on the diagram at points having coordinates that correspond to the derivatives C_{n_β} and C_{l_β} obtained from force tests of the model. The wide band of neutral ratings shows that, over the range covered, the degree of spiral stability or instability was so slight as to make it hard to locate definitely the condition of neutral spiral stability. The ratings indicate that the calculated boundary does define a region of approximately neutral spiral stability.

The tests showed further that the model in a condition of definite spiral instability was not hard to fly. For model configurations that gave definite spiral stability (low vertical-tail area or high dihedral angle), moreover, the detrimental effects of adverse yawing due to aileron deflection were more noticeable than for configurations giving spiral instability. Spiral stability, therefore, does not appear important enough to be attained at the expense of other stability and control characteristics. This statement is especially true for high wing loadings, at which the yawing caused by aileron deflection in a high-dihedral configuration is likely to start or reinforce the lateral oscillation.

Oscillatory stability.- Increasing the value of μ caused a reduction in oscillatory stability, as shown by the qualitative ratings for damping of the oscillations in figure 6. The magnitude of the effects of changes in μ on the damping varied with changes in the model configuration. In general, the greatest effects of μ were noted with the high dihedral angle and small vertical-tail areas, as would be expected from the manner in which the oscillatory-stability boundary ($R = 0$) shifts with increasing values of μ. (See fig. 6.)

The effects of μ on the oscillatory stability with the smallest tail (tail 1) could be determined for only two test conditions because of poor directional-stability characteristics with this tail. The following discussion is therefore concerned only with tails 2, 3, and 4.

At 0° dihedral, the lateral oscillation was practically deadbeat for all values of vertical-tail area and all values of μ. No appreciable reduction in damping with

increase in μ could be noted even with the small vertical tail (tail 2).

At 4° dihedral, the effects of μ on the damping of the oscillation were noticeably greater than at 0° but were not serious for any value of vertical-tail area. At the small values of μ with all vertical tails and even at the highest values of μ with the largest tail, the damping was heavy. Increasing the value of μ caused a sizable reduction in the damping with the small vertical tail (tail 2), but the oscillatory instability indicated by the calculated $R = 0$ boundary was not noted in the flight tests at this condition. (See fig. 6.)

At the 8° and 11° dihedral angles, the effect of μ on the damping of the oscillation was apparent even with the large vertical tail. Increasing μ caused reductions in damping that were sufficient in some cases to cause oscillatory instability. This instability was slight, however, and even for the worst conditions (11° dihedral, tail 2, and $\mu = 31.5$) did not prevent the making of some sustained flights. On the other hand, the instability was considered objectionable in that it introduced considerable difficulty in keeping the wings level with aileron control. This difficulty was caused by a lightly damped rolling motion, which was essentially oscillatory in nature but which was usually started by aileron deflections.

Although insufficient quantitative data were obtained in the flight tests to afford an accurate experimental check of the calculated oscillatory-stability boundaries for the different values of μ, it appears from the ratings of figure 6 that the boundaries were conservative; that is, the calculated boundaries, in general, seemed to exaggerate the detrimental effect of high values of μ on oscillatory stability and some theoretically unstable conditions appeared stable in the flight tests. It should be noted, however, that in no case was the flight behavior for these theoretically unstable conditions considered entirely satisfactory. It therefore appears that, although these particular stability boundaries were not accurate indications of neutral oscillatory stability, they were useful to some extent as indications of conditions of unsatisfactory flight behavior.

Lateral Control

Increasing the value of μ increased the difficulty of maintaining a wing-level attitude with aileron control. In flights with values of μ of 21 and 31.5, attempts to raise a low wing by use of the ailerons usually resulted in a bank in the opposite direction. At times, because of this tendency to overcorrect deviations in bank, several alternate right and left aileron deflections were necessary to return the model to wing-level flight.

It was believed that the tendency to overcontrol with the ailerons was caused principally by the increased moment of inertia in roll, although the fact that higher aileron rolling velocities were obtained at high values of μ probably contributed to the difficulty. The moment of inertia increased in direct proportion to the increase in μ. The rolling velocity due to ailerons increased in direct proportion to the square root of μ. This increase in rolling velocity was caused by the higher airspeeds necessary for flying at the same lift coefficient with the high values of μ.

In an effort to determine which of the two factors - moment of inertia in roll or rolling velocity due to ailerons - was the chief cause of the overcontrol, flights were made at $\mu = 31.5$ with the aileron travel reduced so as to produce smaller rolling velocities. The flights were somewhat smoother, but after large disturbances the tendency to overcontrol when returning to level flight was still present.

In order to verify the indication that moment of inertia was the principal cause of the overcontrol, tests were made with the light model ($\mu = 5.5$) flown at the same airspeed as that used for the flights at $\mu = 31.5$. At this airspeed, which corresponded to a lift coefficient of about 0.2, the ailerons developed the same rolling moments and velocities as in the tests at $\mu = 31.5$, but the flights were much smoother and showed none of the tendencies toward overcontrol that were noted in the flights at heavier loadings. It was thus concluded that increased moment of inertia in roll was the chief cause of the overcontrolling difficulties at the high values of μ.

Although the conclusion that increased moment of inertia in roll caused overcontrolling difficulties was established only for a case in which μ was increased by

increasing wing loading, this fact also holds for the case in which μ is increased by flying at altitude. For an airplane flying at altitude the actual moment of inertia in roll would be the same as at sea level, but the ratio of the moment of inertia in roll to the aerodynamic damping moment opposing roll would be greater because the damping moment varies directly with air density.

General Flight Behavior

The general flight behavior of the model became worse with increasing values of μ, as indicated by the flight-behavior ratings in figure 7. These ratings are indications of the combined effects of all lateral stability and control characteristics on the nature of the flights. It appears from a comparison of the ratings of figure 5 with those of figure 6 that oscillatory stability was the principal factor influencing the pilot's opinion of the general flight behavior of the model in this investigation.

Combinations of vertical-tail area and dihedral angle that gave the best flights at small values of μ usually gave the best flights at higher values of μ. With increasing values of μ, however, the number of model configurations that gave satisfactory flight behavior became progressively smaller. At the low values of μ satisfactory behavior was obtained at all dihedrals with the two large tails (tails 3 and 4) and at the low dihedrals with tail 2. At the highest value of μ, however, satisfactory conditions were obtained only with small dihedral and large tails.

For all values of μ the flight tests indicated that, in general, the best flight behavior was provided by model configurations that had low values of effective dihedral and high values of effective vertical-tail area. With large values of dihedral, the detrimental effects of adverse yawing were usually evident and in some cases the oscillatory stability was poor. With low effective vertical-tail area, the directional stability was poor, as evidenced by excessive yawing motions. The smallest tail (tail 1) did not provide satisfactory directional stability even with 0° dihedral angle, for which the value of C_{n_β} of 0.01 indicated positive stability.

CONCLUSIONS

Based on tests of two similar 1/18-scale dynamic models without propeller in the NACA free-flight tunnel, the following conclusions concerning the effect of wing loading and altitude, or the airplane relative-density factor μ, on lateral stability and control were reached:

1. The value of μ apparently had no effect on spiral stability; this result was in agreement with the calculated spiral-stability boundaries.

2. Increasing the value of μ caused a reduction in oscillatory stability. Although the trend of this reduction was the same as that indicated by the calculated oscillatory-stability boundaries, some flights were possible at conditions well on the unstable side of the calculated boundaries.

3. As μ was increased, the difficulty of maintaining laterally level flight with ailerons became greater.

4. In general, the flight behavior became worse as μ was increased. Satisfactory flight behavior for all loadings was obtained, however, with small dihedral and large vertical-tail area.

Langley Memorial Aeronautical Laboratory,
National Advisory Committee for Aeronautics,
Langley Field, Va.

REFERENCES

1. Bamber, Millard J.: Effect of Some Present-Day Airplane Design Trends on Requirements for Lateral Stability. T.N. No. 814, NACA, 1941.

2. Bryant, L. W., and Pugsley, A. G.: The Lateral Stability of Highly Loaded Aeroplanes. R. & M. No. 1840, British A.R.C., 1938.

3. Shortal, Joseph A., and Osterhout, Clayton J.: Preliminary Stability and Control Tests in the NACA Free-Flight Wind Tunnel and Correlation with Full-Scale Flight Tests. T.N. No. 810, NACA, 1941.

4. Zimmerman, Charles H.: An Analysis of Lateral Stability in Power-Off Flight with Charts for Use in Design. Rep. No. 589, NACA, 1937.

5. Pearson, Henry A., and Jones, Robert T.: Theoretical Stability and Control Characteristics of Wings with Various Amounts of Taper and Twist. Rep. No. 635, NACA, 1938.

TABLE I

VALUES OF DERIVATIVES USED IN STABILITY CALCULATIONS

$\frac{S_v}{S}$	$C_{Y_{\beta(tail)}}$	C_{Y_β}	C_{l_β}	C_{n_β}	C_{l_p}	C_{n_p}	C_{l_r}	C_{n_r}
0	0	-0.310	Dependent variable	-0.025	-0.44	-0.045	0.25	-0.035
.003	-.01	-.320		-.022	-.44	-.045	.25	-.039
.007	-.02	-.330		-.017	-.44	-.045	.25	-.042
.013	-.05	-.360		-.004	-.44	-.045	.25	-.053
.027	-.075	-.385		.006	-.44	-.045	.25	-.062
.037	-.1	-.410		.017	-.44	-.044	.25	-.071
.073	-.2	-.510		.059	-.44	-.043	.25	-.108
.110	-.3	-.610		.102	-.44	-.038	.26	-.144
.146	-.4	-.710		.144	-.44	-.014	.27	-.180

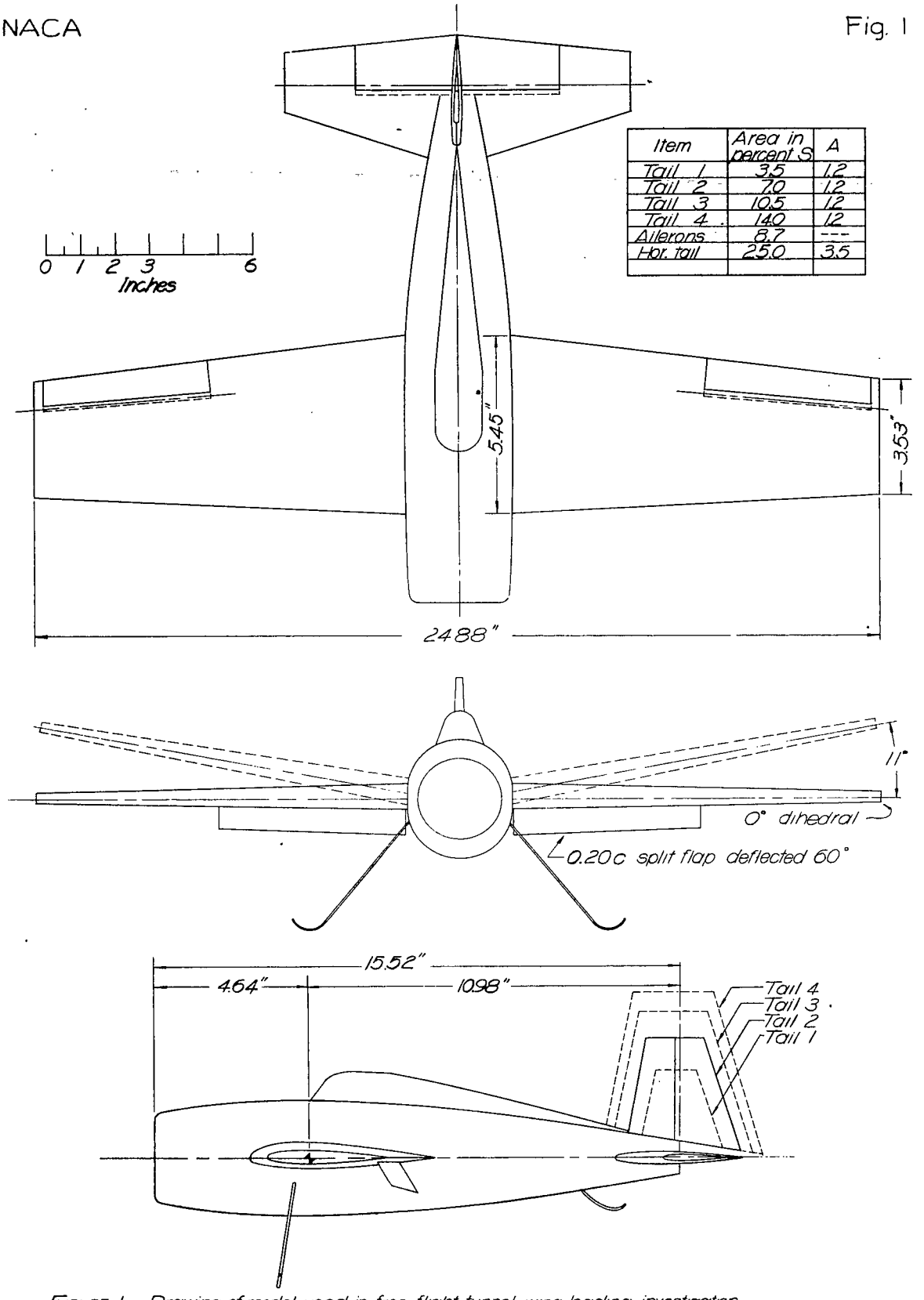

FIGURE 1. – Drawing of model used in free-flight tunnel wing-loading investigation.

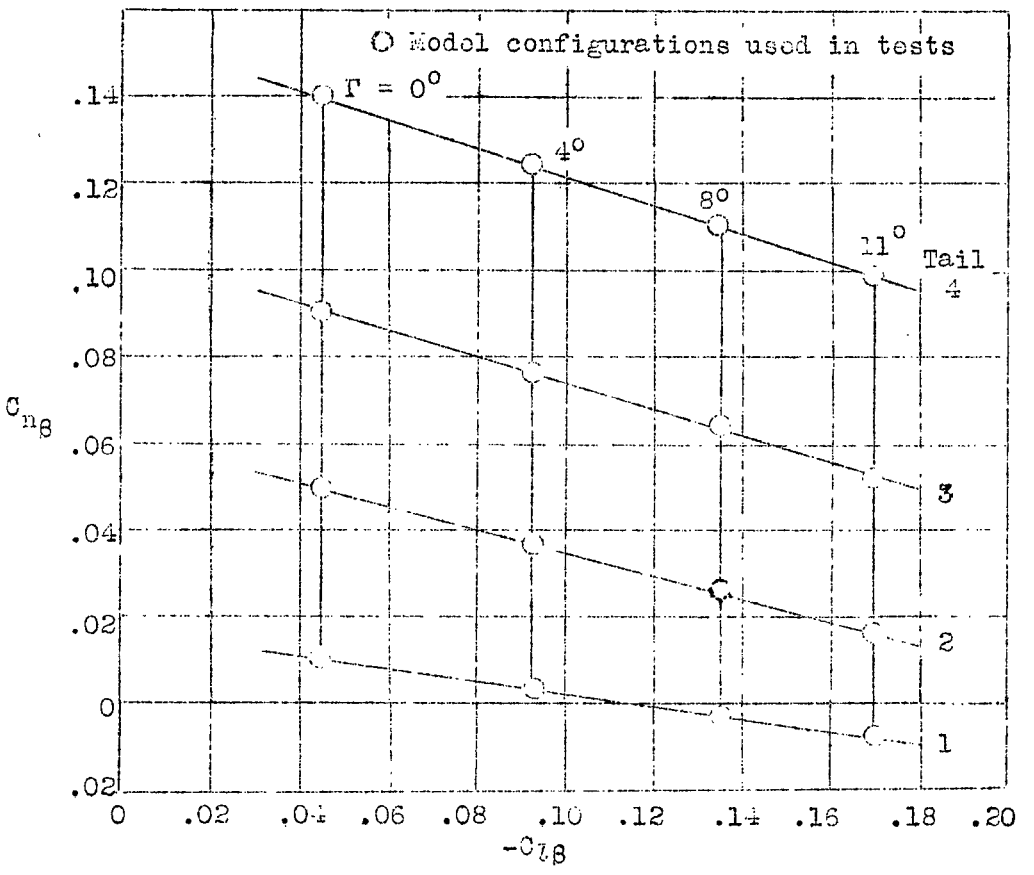

Figure 2.- Values of C_{l_β} and C_{n_β} for the various model configurations used in the tests.

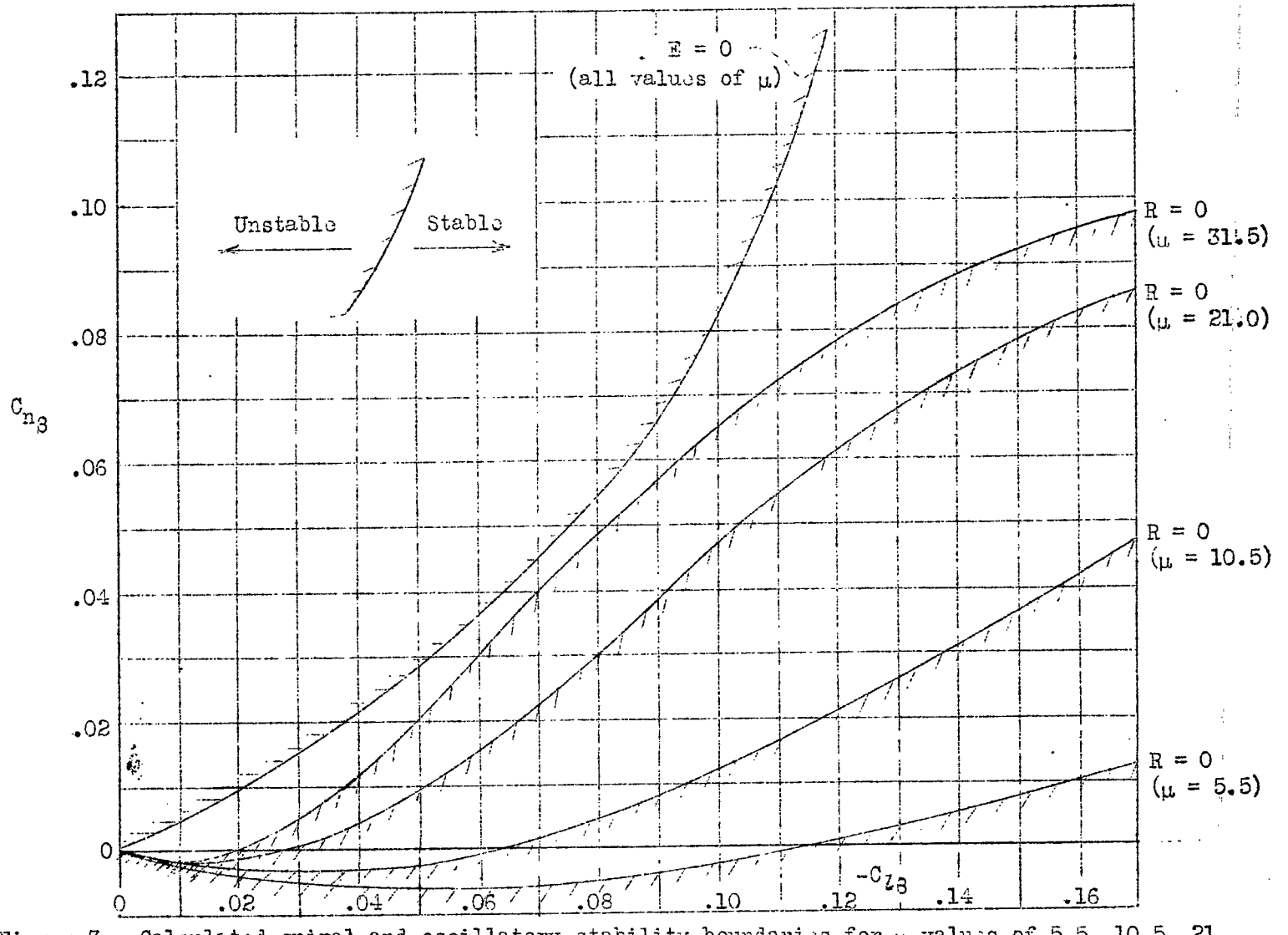

Figure 3.- Calculated spiral and oscillatory stability boundaries for μ values of 5.5, 10.5, 21, and 31.5. C_L = 1.0.

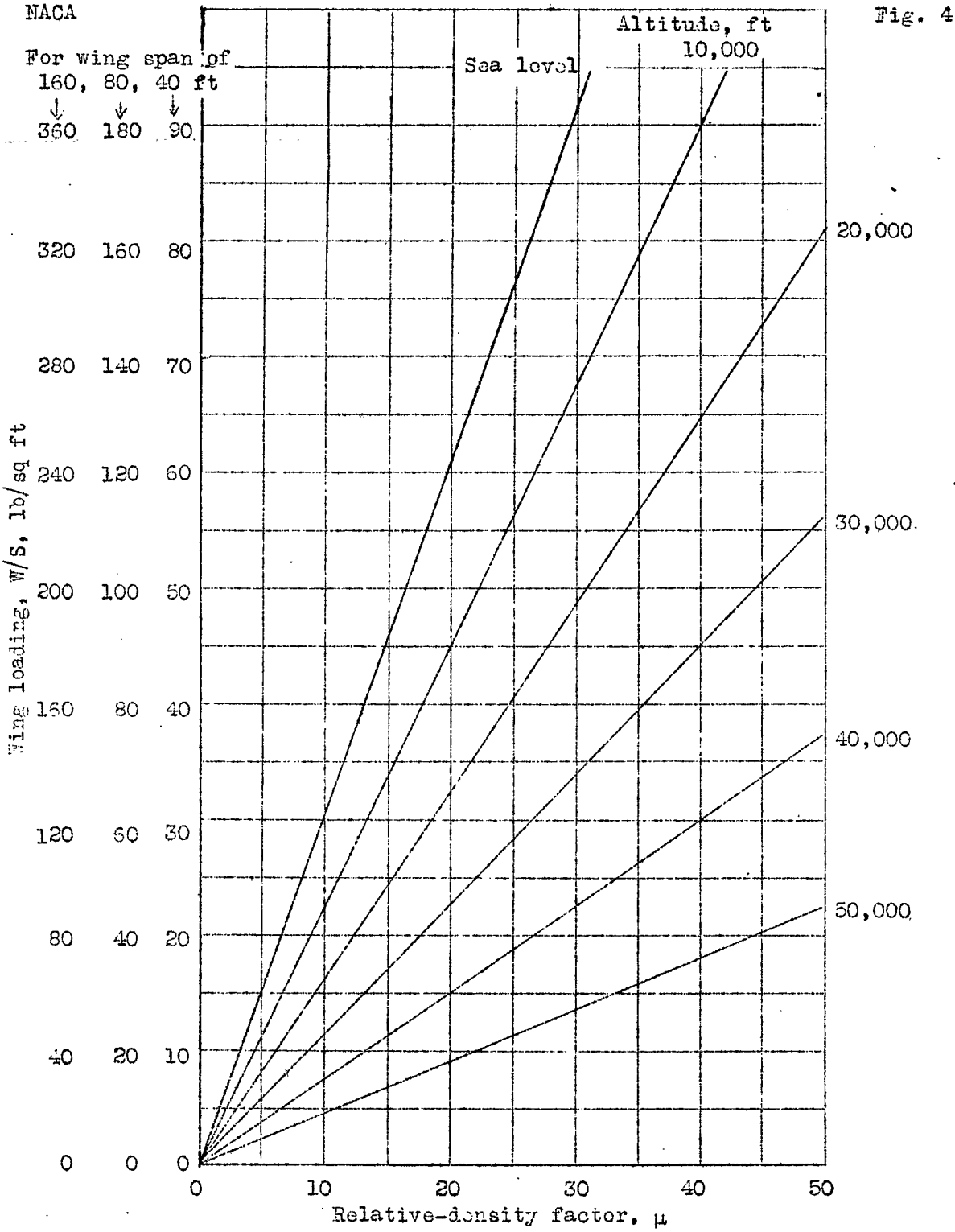

Figure 4.- Variation of μ with wing loading and altitude for various wing spans.

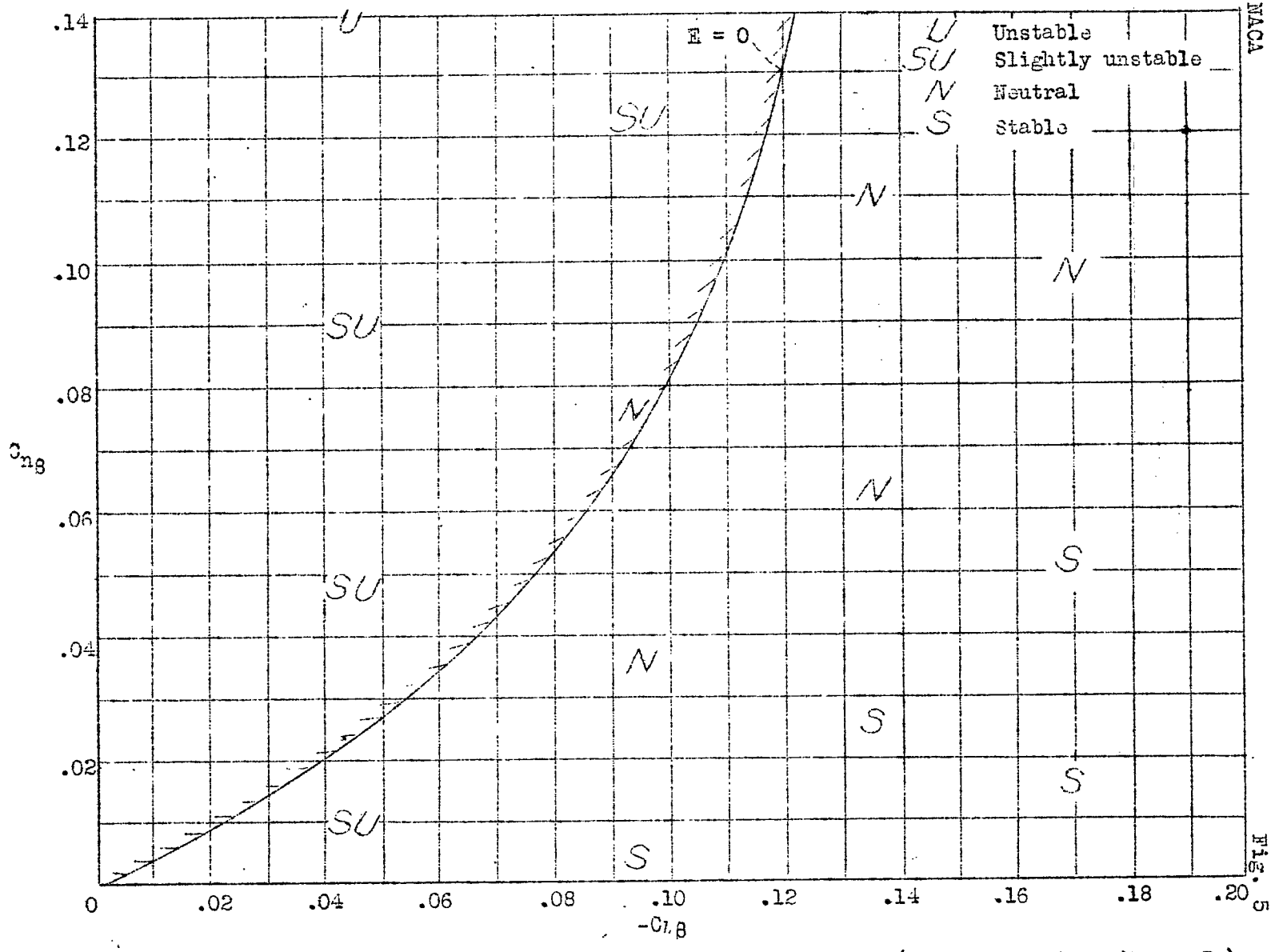

Figure 5.- Spiral-stability ratings for various model configurations. C_L=1.0. (E = 0 curve from figure 3.)

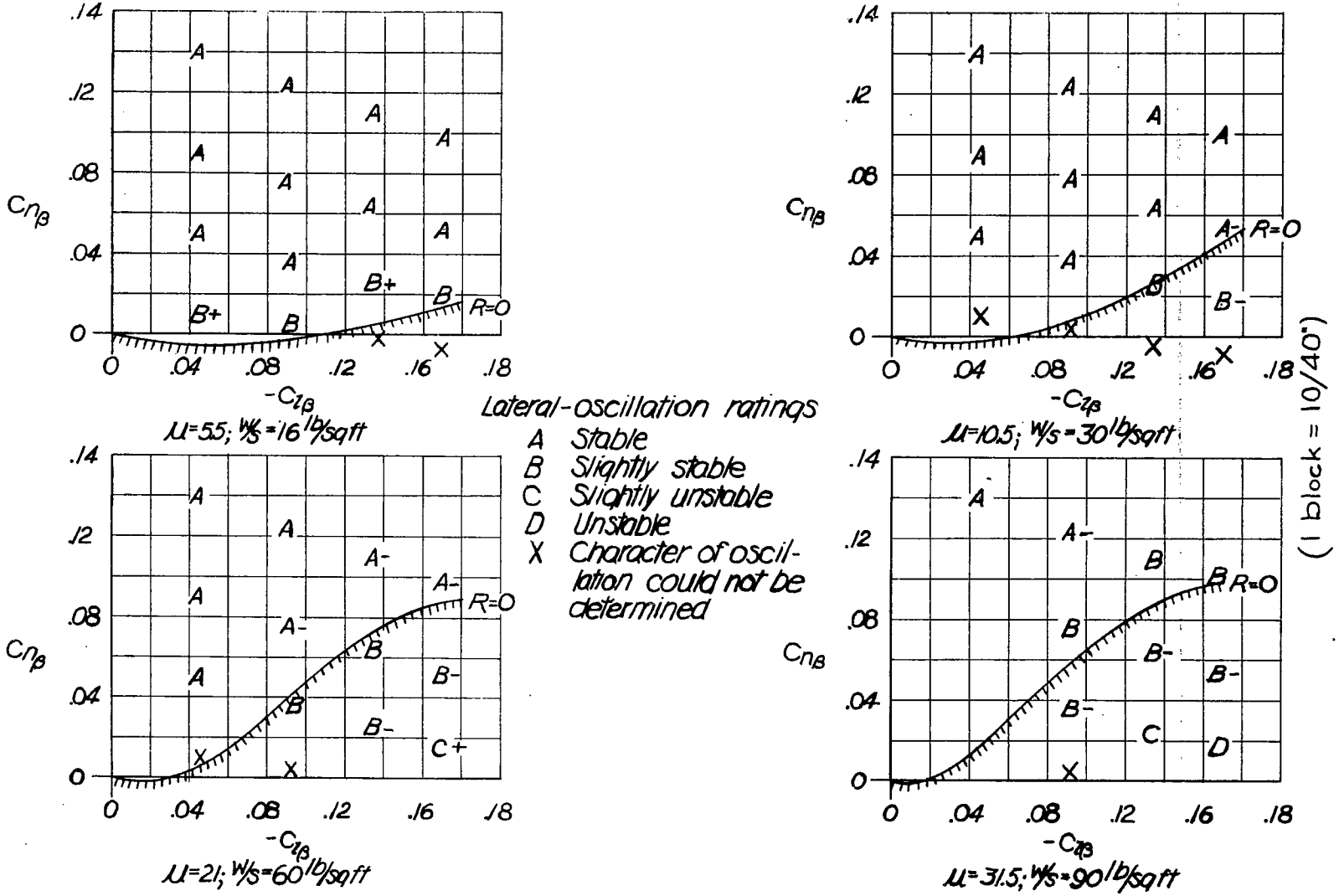

FIGURE 6.- Ratings for damping of lateral oscillation for various wing loadings and model configurations.

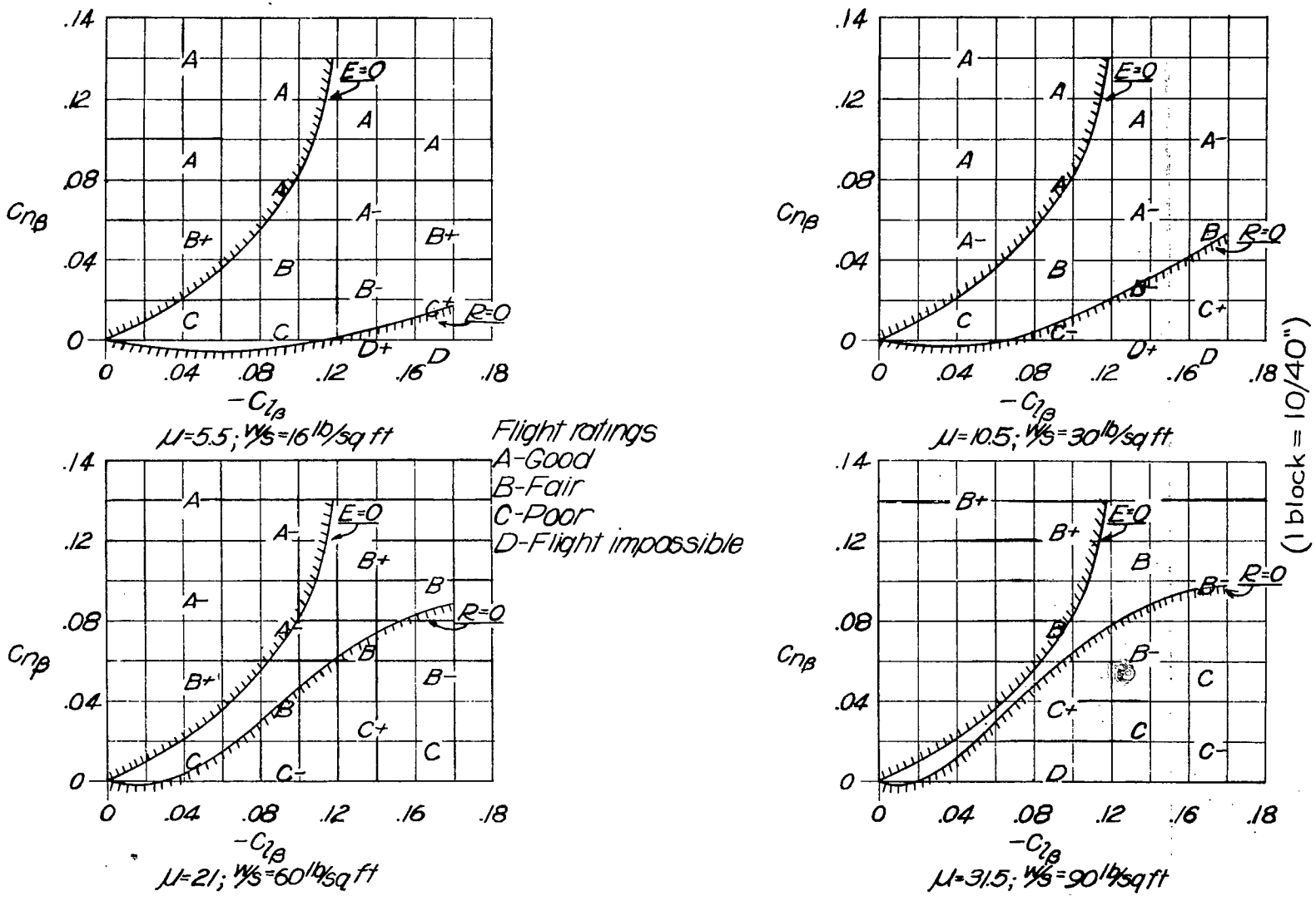

FIGURE 7.- Flight-behavior ratings for various wing loadings and model configurations.

Fig 7